International Journal of Minerals, Metallurgy and Materials
Accepted manuscript, https://doi.org/10.1007/s12613-020-2056-6

Sintering of monoclinic-$SrAl_2Si_2O_8$ ceramics and their immobilization of Sr

Jie Luo[1)], *Xin Li*[1,2)], *Fu-jie Zhang*[1)], *Song Chen*[3)], *and Ding Ren*[1)]

1) Key Laboratory of Radiation Physics and Technology of Ministry of Education, Institute of Nuclear Science and Technology, Sichuan University, Chengdu 610065, China

2) Department of Radiotherapy, Division of Radiation Physics, State Key Laboratory of Biotherapy and Cancer Center, West China Hospital, Sichuan University, Chengdu 610041, China

3) School of Materials Science and Engineering, Southwest Jiaotong University, Chengdu 610031, China

Abstract: Monoclinic $SrAl_2Si_2O_8$ ceramics for the immobilization of Sr were prepared by a liquid-phase sintering method. The sintering temperature, mineral phase composition, microstructure, flexural strength, bulk density, and Sr ions leaching characteristic of $SrAl_2Si_2O_8$ ceramics were investigated. A crystalline monoclinic-$SrAl_2Si_2O_8$ phase was formed by liquid phase sintering at 1223 K. The introduction of four different flux agents (B_2O_3, $CaO \cdot 2B_2O_3$, $SrO \cdot 2B_2O_3$ and $BaO \cdot 2B_2O_3$) to the $SrAl_2Si_2O_8$ ceramics not only reduced the densification temperature and decreased the volatilization of Sr during high-temperature sintering, but also impacted the mechanical properties of the ceramics. The product consistency tests showed that the leaching concentration of Sr ions in sample SAS-B with flux agents B_2O_3 was the lowest and the leaching concentration of Sr ions in sample SAS-B2B with flux agents $BaO \cdot 2B_2O_3$ was the highest. These results show that the leaching concentration of Sr ions depends largely on amorphous phase in the ceramics. Meanwhile, the formation of mineral analog ceramic containing Sr is an important factor to improve the immobilization of Sr.

Keywords: Low temperature liquid-phase sintering; Immobilization of Sr; Monoclinic-$SrAl_2Si_2O_8$; Flux agents

Corresponding author: Ding Ren E-mail: rending2k@scu.edu.cn

1. Introduction

A large amount of liquid waste containing soluble actinide nuclides and fission products with long half-lives, such as ^{137}Cs, ^{90}Sr and ^{79}Se, are generated during the processing of used fuel [1-3]. The concentrated liquid waste becomes high level waste (HLW) after evaporation and is stored in mild steel or stainless-steel tanks [4] as a short-term solution. Ultimately, the HLW will be stored in a deep underground repository for long-term storage based on its solidification and the immobilization of radionuclides [4-6].

In order to adapt the increasing demand for HLW immobilization, new technologies and new materials must be developed [6]. A possible approach is to use the natural analog mineral to immobilize the radioactive waste. HLW can be incorporated into single and multiphase minerals based on the isomorphism of the mineralogy [4,7]. The existence of natural analog minerals in the immobilized forms can effectively provide a solution for the long-term stable geological disposal of radioactive waste [8]. Glass ceramics are a potential material for HLW immobilization because of their high melting point and stability when exposed to radiation [7,9]. Crystalline ceramics can achieve the stable migration of HLW during transportation. Different compositions of glass ceramics can be easily prepared with disposable sintering. Moreover, glass ceramics have a high waste immobilization capacity and density [4]. This confirms their stability for radioactive waste immobilization.

Strontium feldspar ($SrAl_2Si_2O_8$) is a polymorphic mineral similar to natural barium feldspar. Strontium feldspar has two synthetic structures (hexagonal and orthorhombic) and a natural mineral, namely slawsonite. Slawsonite can transform into monoclinic $SrAl_2Si_2O_8$ (Sr-celsian). Sr-celsian has a good phase stability and a high melting point [10]. The mechanical and thermal properties of

monoclinic $SrAl_2Si_2O_8$ (Sr-celsian) are usually better than those of the hexagonal form [11-13]. Hence monoclinic $SrAl_2Si_2O_8$ ceramics are a good candidate for the efficient immobilization of Sr.

However, the high-temperature volatility of radionuclides like ^{90}Sr and ^{137}Cs easily leads to radioactive contamination during sintering [6,7]. Therefore, reasonably regulating the sintering temperature of the ceramic waste form is a great challenge for safe immobilization of HLW. The heat treatment temperature should be lower than 1273 K if Sr is immobilized in the ceramics [7]. To decrease the sintering temperature, liquid phase sintering with different liquid flux agents was performed to form monoclinic $SrAl_2Si_2O_8$ ceramics and simulate the immobilization of ^{90}Sr in monoclinic $SrAl_2Si_2O_8$ ceramics. The sintering behavior of monoclinic $SrAl_2Si_2O_8$ ceramics and the influence of four different flux agents on the immobilization of Sr are discussed in the present work for their possible application in the immobilization of Sr.

2. Experimental

Table 1 and Table 2 show the designed compositions of the ceramic samples and the chemical compositions of kaolin, respectively. The raw materials were $SrCO_3$, H_3BO_3, $Ca(OH)_2$, $Ba(OH)_2 \cdot 8H_2O$, and kaolin. The purity of $SrCO_3$, H_3BO_3, $Ca(OH)_2$, and $Ba(OH)_2 \cdot 8H_2O$ was higher than 99 %. Since the activation of kaolin helps the chemical combination of the alkali earth ions with SiO_2 and Al_2O_3 during sintering, it was calcined at 1073 K for 3 hours to obtain meta-kaolin ($Al_2O_3 \cdot 2SiO_2$) [14,15].

Table 1. Chemical compositions of monoclinic-$SrAl_2Si_2O_8$ ceramics

Sample	Designed compositions	
	Pre-sintered ceramic powders	Flux agents
SAS-B	85wt% $SrAl_2Si_{2.3}O_{8.6}$	15wt% B_2O_3
SAS-S2B	80wt% $SrAl_2Si_{2.3}O_{8.6}$	20wt% $SrO{\cdot}2B_2O_3$
SAS-C2B	80wt% $SrAl_2Si_{2.3}O_{8.6}$	20wt% $CaO{\cdot}2B_2O_3$
SAS-B2B	80wt% $SrAl_2Si_{2.3}O_{8.6}$	20wt% $BaO{\cdot}2B_2O_3$

Table 2. Chemical compositions of kaolin / wt%

Kaolin	Loss	SiO_2	Al_2O_3	Fe_2O_3	CaO	MgO	SO_3	K_2O	Na_2O	P_2O_5	Total
Mass	7.55	51.68	39.05	1.15	0.48	0.21	0.19	0.18	0.13	0.27	100.89

The process to prepare $SrAl_2Si_2O_8$ ceramic samples is shown in Fig. 1. $SrCO_3$ and meta-kaolin powders were weighed according to the designed scheme and ball-milled with deionized water for 3 hours. Subsequently, we pre-sintered the dried powders at 873 K for 6 hours to obtain the ceramic powders. The flux agents (borate compounds) were added to the pre-sintered ceramic samples and milled with deionized water to obtain uniform slurries so that the densification sintering at relatively low temperatures can be achieved. The raw materials used for the preparation of the borate flux agents were $Ca(OH)_2$, $SrCO_3$, $Ba(OH)_2{\cdot}8H_2O$ and H_3BO_3 with mass ratios corresponding to the designed chemical formula. The mixed powders were molded after the slurries were dried. Finally, the molded green bodies were continuously sintered at 873 K for 3 hours and at 1223 K for 2 hours to obtain the monoclinic $SrAl_2Si_2O_8$ ceramic samples.

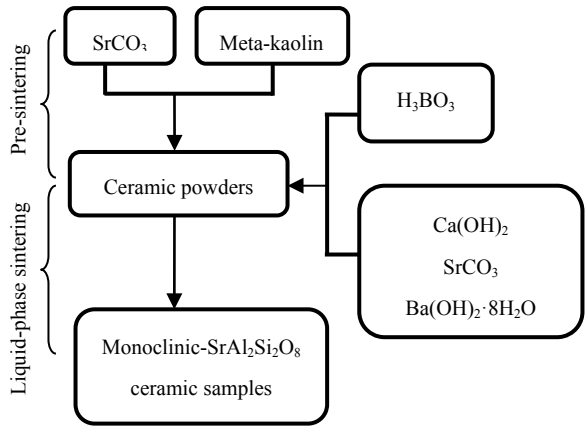

Fig. 1. Brief preparation process of $SrAl_2Si_2O_8$ ceramics samples.

The thermogravimetric and differential scanning calorimetry (TG-DSC) curves of the flux agents were systematically recorded (NETZSCH STA449C, Germany). The surface morphology was analyzed using field emission scanning electron microscopy (SEM, JEOL JSM-7500F, Japan) and the crystalline phases of the ceramic samples were measured by powder X-ray diffraction (XRD, EMPYREAN, Holland). The bulk density and flexural strength of samples were measured using the Archimedes method and a three-point bending test, respectively. The ion leaching tests, referred to as the product consistency test (PCT) method A, were carried out according to ASTM C1285-14 [16]. After ceramic samples were grounded, 1 g of powder with 100 - 200 mesh was placed in a polytetraflfluoroethylene vessel. Then, deionized water was added to the vessel with a mass ratio of deionized water to the powder of 10. Subsequently, the polytetraflfluoroethylene vessel was sealed in a stainless vessel and placed in an oven at 363 K for 168 ± 1 hours. The concentration of ions in the leachate was measured using an inductively-coupled plasma optical emission spectrometer (ICP-OES 5100 SVDV, Agilent).

3. Results and discussion

3.1. The thermogravimetric and differential scanning calorimetry curves of the flux agent

slurries

Fig. 2 shows the thermogravimetric and differential scanning calorimetry curves of the flux agent slurries. The weight of the flux agent slurries decreased quickly due to the evaporation of water and the volatilization of excess B_2O_3 when temperature was below 700 K. The water evaporation led to heat absorption with peaks near 400 K, labeled as A. The abundant water originated from the residual deionized water, the chemical reactions, and the water embedded in the crystalline structure. However, the DSC curves were primarily dominated by the exothermic process from borate. The weight decreased slowly when the temperature increased, which was attributed to the decomposition of hydroxides and carbonates. The exothermic peak appeared between 950 K and 1100 K and was labeled as B. The borate compounds gradually melted when temperature increased, and a liquid phase was finally formed by the slow endothermic reactions. The liquid phase sintering temperature depends on the low melting characteristic of the flux agents. Additionally, the phase diagrams of $CaO\text{-}B_2O_3$, $SrO\text{-}B_2O_3$, and $BaO\text{-}B_2O_3$ show that their liquid phases exist below 1223 K [17-19]. Therefore, we chose a temperature of 1223 K for the liquid phase sintering temperature of monoclinic $SrAl_2Si_2O_8$ ceramics since it is a little higher than the temperature of liquid phases according to the TG-DSC curves and phase diagrams.

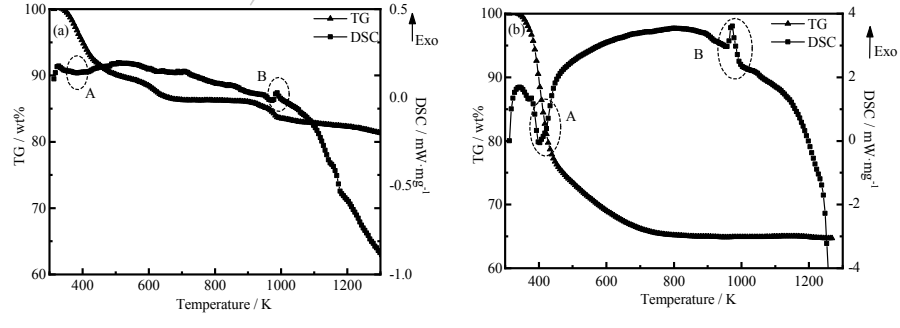

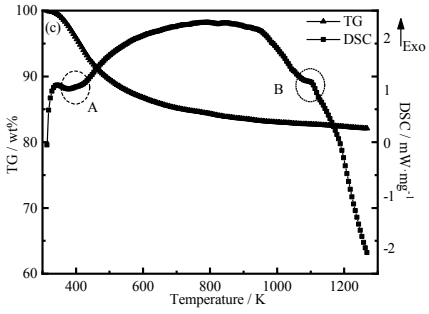

Fig. 2. The thermogravimetric and differential scanning calorimetry (TG-DSC) curves of the flux agent slurries: (a) $SrO{\cdot}2B_2O_3$; (b) $CaO{\cdot}2B_2O_3$; (c) $BaO{\cdot}2B_2O_3$.

3.2. Microstructures and mechanical properties

Fig. 3 shows the microstructure of $SrAl_2Si_2O_8$ ceramic samples. The bulk density, flexural strength, and apparent porosity of samples are listed in Table 3. Fig. 3 indicates that the grains are surrounded by a glassy phase. The grain size of the ceramic sample SAS-B is the biggest. During the sintering process, the grain interspace and the pores of the ceramics are gradually permeated and filled by the liquid phase because of the low melting point of the flux agents, which makes the microstructure of the $SrAl_2Si_2O_8$ ceramics gradually more compact. When the borate flux agent is used as the liquid phase medium, it promotes the dispersion and the combination of various particles and forms mineral phases with a high thermodynamic stability during sintering according to the classical theory of liquid phase sintering [20]. The bulk density and the flexural strengths of the ceramic samples (Table 3) are significantly improved when the apparent porosity decreases. During liquid phase sintering, the addition of the flux agents helps the densification of the $SrAl_2Si_2O_8$ ceramic. In addition, replacement reactions occur between the alkali earth ions due to the presence of Ca and Ba ions in the flux agents and because Ca and Ba in the flux agents have similar physical and chemical characteristics as Sr. These reactions also influence the formation of the phase

structure and the immobilization of Sr.

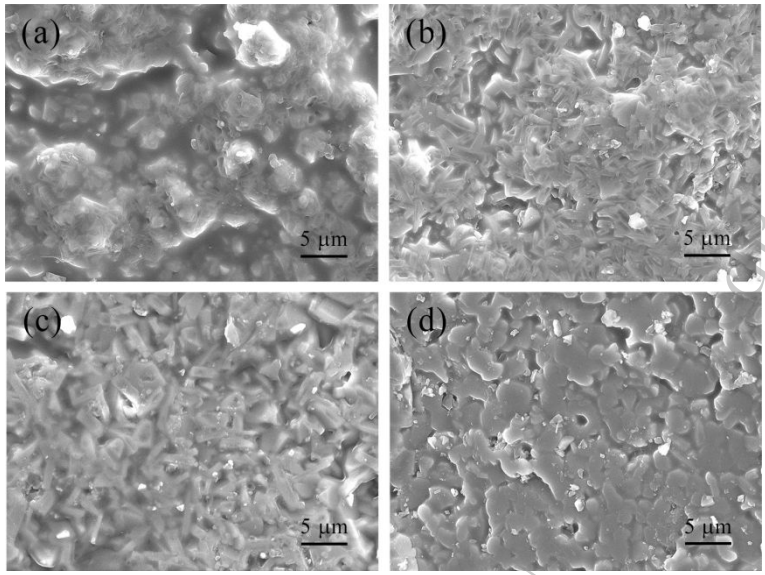

Fig. 3. SEM images of $SrAl_2Si_2O_8$ ceramic samples: (a) SAS-B; (b) SAS-S2B; (c) SAS-C2B; (d) SAS-B2B.

Table 3. Mechanical properties of $SrAl_2Si_2O_8$ ceramic samples

Sample	Bulk density / ($g \cdot m^{-3}$)	Flexural strength / (Mpa)	Apparent porosity / vol%
SAS-B	2.540±0.076	30±3.0	1.46±0.12
SAS-S2B	2.800±0.084	45±4.5	0.58±0.05
SAS-C2B	2.570±0.077	33±3.3	0.71±0.06
SAS-B2B	3.020±0.091	60±6.0	0.52±0.04

3.3. XRD Patterns of the $SrAl_2Si_2O_8$ ceramics

Fig. 4 shows the XRD patterns of the $SrAl_2Si_2O_8$ ceramic samples obtained at 1223 K using the liquid phase sintering method. The major phase of samples SAS-B, SAS-S2B, and SAS-C2B is a monoclinic $SrAl_2Si_2O_8$ phase and a small amount of $CaAl_2Si_2O_8$ phase is present in SAS-C2B. The

monoclinic $SrAl_2Si_2O_8$ phase is a typical and important strontium feldspar phase. The emergence of $CaAl_2Si_2O_8$ phase in ceramics means that the phase composition of $SrAl_2Si_2O_8$ ceramics was changed because Sr was substituted by Ca. The XRD patterns also show that the major phase of SAS-B2B sample is a monoclinic $Ba_{0.25}Sr_{0.75}Al_2Si_2O_8$ phase. Ba element effectively participates in the physical and chemical growth of $Ba_{0.25}Sr_{0.75}Al_2Si_2O_8$ crystal via a monoclinic polymorph of the (Ba, Sr)$Al_2Si_2O_8$ solid solution during sintering [10]. The substitution of Sr by Ca and Ba results in a reduced incorporation of Sr into the mineral phase and more Sr ions in the amorphous phase.

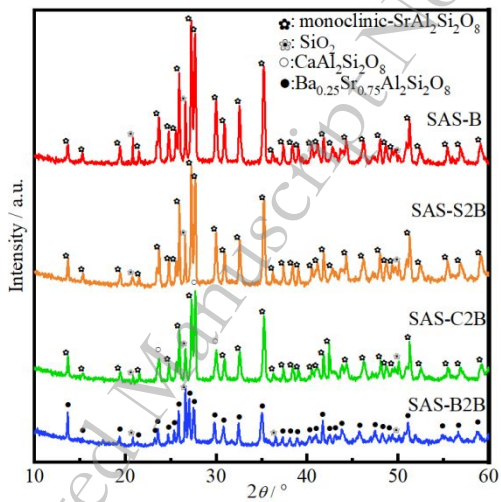

Fig. 4. XRD patterns of $SrAl_2Si_2O_8$ ceramic samples SAS-B, SAS-S2B, SAS-C2B and SAS-B2B.

Usually, the low-temperature densification of ceramic materials with high melting points largely depends on the fusion between the ceramic powders and the low-melting flux agents, which constitutes the liquid-phase sintering process [14,21,22]. To obtain $SrAl_2Si_2O_8$ ceramics, the chemical components of the flux agents and $SrAl_2Si_2O_8$ need to be in the same range. The phase diagrams of low-melting binary compositions like $SrO\text{-}B_2O_3$, $CaO\text{-}B_2O_3$ and $BaO\text{-}B_2O_3$ show that

these compositions yield to the formation of a liquid phase at a relatively low sintering temperature. The borate compounds and their precursors are formed from the aqueous milling route of the raw materials [23,24]. Consequently, there are liquid phases to help the formation of the monoclinic $SrAl_2Si_2O_8$ ceramics at low temperatures due to the presence of low-melting borate flux agents during sintering. Therefore, the addition of the borate flux agents containing alkali earth metals is crucial to reduce the sintering temperature of the monoclinic $SrAl_2Si_2O_8$ ceramics via a liquid phase sintering approach.

The XRD patterns show that a SiO_2 phase is also present. The formation of SiO_2 is attributed to the excess of SiO_2 in meta-kaolin. The molar ratio of SiO_2 to Al_2O_3 is 2 in the ideal molecular formula, but the ratio of the raw materials was 2.3, as listed in Table 2. The excessive SiO_2 is not completely consumed during sintering and a SiO_2 phase appeared in the XRD patterns.

3.4. Ion leaching behavior

The leaching behaviors of the major ions present in the $SrAl_2Si_2O_8$ ceramic samples was studied using leaching tests referenced to PCT-A. The normalized data are listed in Table 4 and the leaching concentration of each element is calculated by equation (1) [16]:

$$C_i(\text{sample}) = \frac{C_i(n) \cdot V_f(n)}{V_i(n)} - C_i(\text{blank}) \quad (1)$$

Where $C_i(n)$ is the concentration of element "i" numbered n, $V_i(n)$ is the initial volume of leachate numbered n, $V_f(n)$ is the final volume of the leachate numbered n, and n is the number of the replicate sample. C_i(blank) is the average concentration of the blank samples. The normalized elemental concentration is calculated by equation (2) [16]:

$$NC_i = \frac{C_i(\text{sample})}{f_i} \quad (2)$$

Where NC_i is the normalized concentration, C_i(sample) is the modified concentration of element "i", and f_i is the mass fraction of element "i" in the un-leached sample.

Table 4. The normalized elemental concentration (NC_i) of samples on PCT

Sample	n	NC_i / (g·L^{-1})					pH
		Sr	Al	B	Ca	Ba	
SAS-B	1	0.552	0.017	3.186			8.42
	2	0.583	0.015	5.872			8.43
	3	0.602	0.014	4.393			8.38
SAS-S2B	1	2.322	0.020	14.957			9.22
	2	2.268	0.021	13.932			9.24
	3	2.304	0.022	14.532			9.21
SAS-C2B	1	3.158	0.019	12.092	6.329		9.18
	2	3.133	0.021	11.750	6.158		9.19
	3	3.143	0.018	11.975	6.143		9.15
SAS-B2B	1	14.755	0.027	24.310		3.673	10.78
	2	17.470	0.070	27.431		4.697	11.18
	3	15.695	0.054	25.641		3.835	10.92

The experimental data show that the leaching concentration of Al ions is very low, even though Al is the main element in the formation of the mineral phases. This indicates that the leaching of ions mainly comes from amorphous phases and mineral phases have a great influence on the immobilization of ions. There is a glassy phase in samples due to the liquid sintering. The leaching

of ions is usually related to the ions exchanged between glassy phase and leachate. Some alkali earth ions, such as Ca, Sr and Ba, are chemically bonded with Si-O networks, but it is also possible for the alkali earth ions to leach from glassy phase into leachate if Si-O-Me (Me=Ca, Sr and Ba) network is broken due to the meta-stability of glassy phase and especially because of a poor alkali resistance of glassy phase [25]. Then, ~~the~~ ions are easily spread and migrated in hydrothermal conditions. Once ions are leached into leachate, the alkali earth ions lost in glassy phase are supplemented by other alkali earth ions or hydrogen ions in the aqueous solution [25]. The leaching concentration of Sr in SAS-B is the lowest. In the XRD patterns of samples, the intensity of the peak for monoclinic-$SrAl_2Si_2O_8$ phase in SAS-B is stronger than the ones in SAS-C2B and SAS-B2B. This also indicates that the immobilization properties of samples mainly depend on the crystalline mineral phase whereas the leaching concentration of ions is related to amorphous phase. Although the flux agents containing alkali earth ions help decrease sintering temperature and improve mechanical properties of ceramics (Fig. 2 and Table 3), the leaching concentration of Sr ions in SAS-S2B, SAS-C2B, and SAS-B2B is higher than that in SAS-B. The increase of Sr leaching concentration in SAS-C2B and SAS-B2B with the addition of Ca and Ba ions, respectively, correlates with the decrease of the intensity of the peaks for monoclinic $SrAl_2Si_2O_8$ phase in the XRD patterns. The reduction of the immobilization for Sr ions is related to the replacement reactions between the alkali earth ions during sintering. The leaching concentration of Sr ions in SAS-S2B is higher than that in SAS-B, which shows that the Sr content in samples affects the leaching concentration of Sr in the leachates. Due to the addition of $SrO{\cdot}2B_2O_3$ in SAS-S2B, the excess Sr is not completely incorporated into $SrAl_2Si_2O_8$ phase and Sr ions are present in amorphous phase, which increases the leaching concentration of Sr ions. The leaching concentration

of Sr ions in SAS-B2B is the highest. The XRD patterns show that the main crystalline phase of SAS-B2B is $Ba_{0.25}Sr_{0.75}Al_2Si_2O_8$. There are more Sr ions in amorphous phase and, consequently, Sr ions leaching concentration is the highest. Overall, Sr immobilization efficiency in the crystalline ceramic depends largely on the formation of the Sr mineral structure.

4. Conclusions

The sintering behavior and immobilization of Sr ions after adding four flux agents to monoclinic $SrAl_2Si_2O_8$ ceramics have been investigated. The results indicated that monoclinic $SrAl_2Si_2O_8$ ceramics are formed at 1223 K when assisted by the borate flux agents during sintering, which decrease the volatilization of Sr at high sintering temperatures. Additionally, the presence of monoclinic $SrAl_2Si_2O_8$ phase was important for the crystalline ceramic to immobilize Sr ions efficiently. The PCT leaching results indicated that the immobilization of Sr in sample SAS-B was better than that in samples with other flux agents. The immobilization of Sr by a low-temperature liquid-phase sintering method highly depends on the mineral phase of Sr. In particular, the formation of strontium feldspar structures is important to obtain a good immobilization of Sr ions.

Acknowledgements

This work was supported by the National Natural Science Foundation of China [grant number 11605116].

References

[1] T. Hijikata, M. Sakata, H. Miyashiro, K. Kinoshita, T. Higashi, and T. Tamai, Development of pyrometallurgical partitioning of actinides from high-level radioactive waste using a reductive extraction step, *Nucl. Technol.*, 115(1996) No. 1, p. 114.

[2] G.R. Choppin, Actinide speciation in the environment, *J. Radioanal. Nucl. Chem.*, 273(2007),

No. 3, p. 695.

[3] M.Y. Alyapyshev, V.A. Babain, and Y.A. Ustynyuk, Recovery of minor actinides from high-level wastes: modern trends, *Russ. Chem. Rev.*, 85(2016), No. 9, p. 943.

[4] C.M. Jantzen, W.E. Lee, and M.I. Ojovan, Radioactive waste conditioning, immobilization, and encapsulation processes and technologies: overview and advances, [in] *Radioactive Waste Management and Contaminated Site Clean-up: Processes, Technologies and International Experience*. Woodhead, Cambridge, 2013, p. 171.

[5] R.S. Forsyth and L.O. Werme, Spent fuel corrosion and dissolution, *J. Nucl. Mater.*, 190(1992), p. 3.

[6] I.W. Donald, B.L. Metcalfe, and R.N.J. Taylor, The immobilization of high level radioactive wastes using ceramics and glasses, *J. Mater. Sci.*, 32(1997), No. 22, p. 5851.

[7] L. Wang and T. Liang, Ceramics for high level radioactive waste solidification, *J. Adv. Ceram.*, 1(2012), No. 3, p. 194.

[8] W. E. Lee, M. I. Ojovan, M. C. Stennett, and N. C. Hyatt, Immobilization of radioactive waste in glasses glass composite materials and ceramics, *Adv. Appl. Ceram.*, 105(2006), No. 1, p. 3.

[9] E.R. Vance, B.D. Begg, and D.J. Gregg, Immobilization of high-level radioactive waste and used nuclear fuel for safe disposal in geological repository systems, [in] J. Ahn and M.J. Apted, eds., *Geological Repository Systems for Safe Disposal of Spent Nuclear Fuels and Radioactive Waste*, Woodhead, Cambridge, 2017, p. 269.

[10] C. Ferone, B. Liguori, A. Marocco, S. Anaclerio, M. Pansini, and C. Colella, Monoclinic (Ba, Sr)-celsian by thermal treatment of (Ba, Sr)-exchanged zeolite A, *Microporous Mesoporous Mate.*, 134(2010), No. 1-3, p. 65.

[11] C.M. López-Badillo, J. López-Cuevas, C.A. Gutiérrez-Chavarría, J.L. Rodríguez-Galicia, and M.I. Pech-Canul, Synthesis and characterization of $BaAl_2Si_2O_8$ using mechanically activated precursor mixtures containing coal fly ash, *J. Eur. Ceram. Soc.*, 33(2013), No. 15-16, p. 3287.

[12] Y. Kobayashi and M. Inagaki, Preparation of reactive Sr-celsian powders by solid-state reaction and their sintering, *J. Eur. Ceram. Soc.*, 24(2004), No. 2, p. 399.

[13] B. Liguori, C. Ferone, S. Anaclerio, and C. Colella, Monoclinic Sr-celsian by thermal treatment of Sr-exchanged zeolite A, LTA-type framework, *Solid State Ionics*, 179(2008), No. 40, p. 2358.

[14] S. Chen, D.G. Zhu, and X.S. Cai, Low-temperature sintering behavior and properties of monoclinic-$SrAl_2Si_2O_8$ ceramics prepared via an aqueous suspension milling process, *J. Mater. Sci. - Mater. Electron.*, 27(2016), No. 11, p. 11127.

[15] Z.H. Xu, Z. Jiang, D.D. Wu, X. Peng, Y.H. Xu, N. Li, Y.J. Qi, and P. Li, Immobilization of strontium-loaded zeolite A by metakaolin based-geopolymer, *Ceram. Int.*, 43(2017), No. 5, p. 4434.

[16] ASTM International C 1285-14, Standard Test Methods for Determining Chemical Durability of Nuclear, Hazardous, and Mixed Waste Glasses and Multiphase Glass Ceramics The Product Consistency Test (PCT).

[17] E.M. Levin, H.F. McMurdie, M.K. Reser (Eds.), *Phase diagrams for ceramists*, The American Ceramic Society, Columbus, 1956.

[18] E.M. Levin and H.F. McMurdie, The system $BaO-B_2O_3$. *J. Am. Ceram. Soc.*, 32(2006), No. 3, p. 99.

[19] H. Witzmann and G. Herzog, Luminescence-optical behavior of alkaline earth borate luminophors. *Z. Phys. Chem.*, 225(1964), p. 197.

[20] R.M. German, S. Farooq, and C.M. Kipphut, Kinetics of liquid sintering, *Mater. Sci. Eng., A*,

105-106(1988), p. 215.

[21] S. Chen, D.G. Zhu, and X.S. Cai, Low-Temperature Densification Sintering and Properties of Monoclinic-$SrAl_2Si_2O_8$ Ceramics, *Metall. Mater. Trans. A*, 45(2014), No. 9, p. 3995.

[22] S. Rajesh and H. Jantunen, Low Temperature Sintering and Dielectric Properties of Alumina-Filled Glass Composites for LTCC Application, *Int. J. Appl. Ceram. Tec.*, 9(2012), No. 1, p. 52.

[23] S.D. Ross and M. Finkelstein, *Barium borate preparation*, United States Patent, Appl.4897249,1990.

[24] S. Chen, D.G. Zhu, P.Q. Sun, and H.L. Sun, Sintering behavior and dielectric properties of $SrB_2Si_2O_8$ ceramics. *J. Mater. Sci. Mater. Electron.*, 24(2013), No.11, p. 4593.

[25] H. Scholze, *Glass*, Springer, New York, 1991.